Journal of
Materials Chemistry C

PAPER

View Article Online
View Journal

Cite this: DOI: 10.1039/c5tc01967b

Quantitative real time sensing reveals enhanced sensitivity of polar dendrimer thin films for plastic explosive taggants†

Andrew J. Clulow,[a] Hamish Cavaye,[a] Guoqiang Tang,[a] Paul E. Shaw,[a] Justin J. Cooper-White,[bc] Paul L. Burn*[a] and Paul Meredith[a]

Received 2nd July 2015,
Accepted 6th August 2015

DOI: 10.1039/c5tc01967b

www.rsc.org/MaterialsC

A method of introducing pulses of analyte vapours has been developed to study the interactions of nitro-containing analytes with fluorescent sensing films. The quenching of the photoluminescence of thin dendrimer films by exposure to sub-saturation concentration vapour pulses of nitro-containing analytes is quantified and the reversibility of quenching interactions qualitatively examined. The analysis reveals a linear dependence of the initial/quenched fluorescence ratio (F_0/F) with quencher concentration akin to Stern–Volmer behaviour routinely used to quantify quenching efficiency in solution. Detection limits and quenching efficiencies were calculated in the sub-saturation regime for each of the analytes and trace-level detection of 1,4-dinitrobenzene, 2,4-dinitrotoluene, 4-nitrotoluene, and nitromethane vapours was observed. It was found that the sensitivity of first generation bifluorene- and carbazole-cored dendrimers towards vapours of the nitroaliphatic taggant 2,3-dimethyl-2,3-dinitrobutane was significantly enhanced by changing the solubilising chains on the core from alkyl to oligo(ethylene oxide) groups. The responses of the films were observed to be independent of film exposure history making these dendrimers interesting candidates for deployment in thin film vapour sensors for explosives.

Introduction

The need to detect high explosives in current and past conflict zones has spurred the development of new sensing technologies.[1–4] Nitroaromatics are common targets for detection due to the widespread use of 2,4,6-trinitrotoluene (TNT) in military explosive compositions and landmines.[5–8] Nitroaliphatic compounds, whilst having received comparably less attention than nitroaromatics, are also important targets for the detection of explosives due to their use as tagging agents [*e.g.*, 2,3-dimethyl-2,3-dinitrobutane (DMNB)] and accelerants in explosive mixtures.[9–12] Amongst the technologies developed for explosives detection, oxidative quenching of fluorescent thin films has come to the fore as a promising method for portable detection of nitrated organic vapours. As a consequence there has been a steady stream of new fluorescent organic sensing molecules reported,[7,13–24] although the focus of these studies has generally been on the detection of nitroaromatic analytes. One of the reasons why DMNB is less well studied is that it has a lower electron affinity than the nitroaromatics and hence is more difficult to detect.[13] Initial work on fluorescent sensing materials focussed on conjugated polymers, and indeed polymeric-based materials have remained the mainstay of materials development. However, more recently fluorescent dendrimers have been used for the detection of both nitroaromatic and nitroaliphatic analytes.[25–30] Fluorescent dendrimers are comprised of a core, dendrons, and surface groups, and this modular nature makes them an ideal class of materials to explore different sensing concepts. For example, it has been shown previously that dendrimers with carbazole-containing cores displayed a larger response to DMNB in solution compared to a dendrimer with a bifluorenyl core but the same dendrons and surface groups.[29]

Typically, the organic sensing molecules possess lipophilic alkyl chains that make the conjugated chromophores soluble in organic solvents and enable them to be processed to form thin films. However, nitrated organics are inherently polar molecules due to the electron withdrawing nature of the nitro groups. In this work we explore the effect of replacing the non-polar alkyl chains typically found on fluorescent dendrimers with more polar groups. 2-(2-Methoxyethoxy)ethyl chains were chosen as the polar groups as poly(ethyleneoxide)s are used as polar stationary

[a] Centre for Organic Photonics & Electronics, The University of Queensland, St Lucia, QLD 4072, Australia. E-mail: p.burn2@uq.edu.au
[b] Australian Institute for Bioengineering and Nanotechnology, The University of Queensland, St Lucia, QLD 4072, Australia
[c] School of Chemical Engineering, The University of Queensland, St Lucia, QLD 4072, Australia

† Electronic supplementary information (ESI) available: The experimental details for the synthesis and characterisation of the dendrimer precursors **1** and **3b** is detailed. See DOI: 10.1039/c5tc01967b

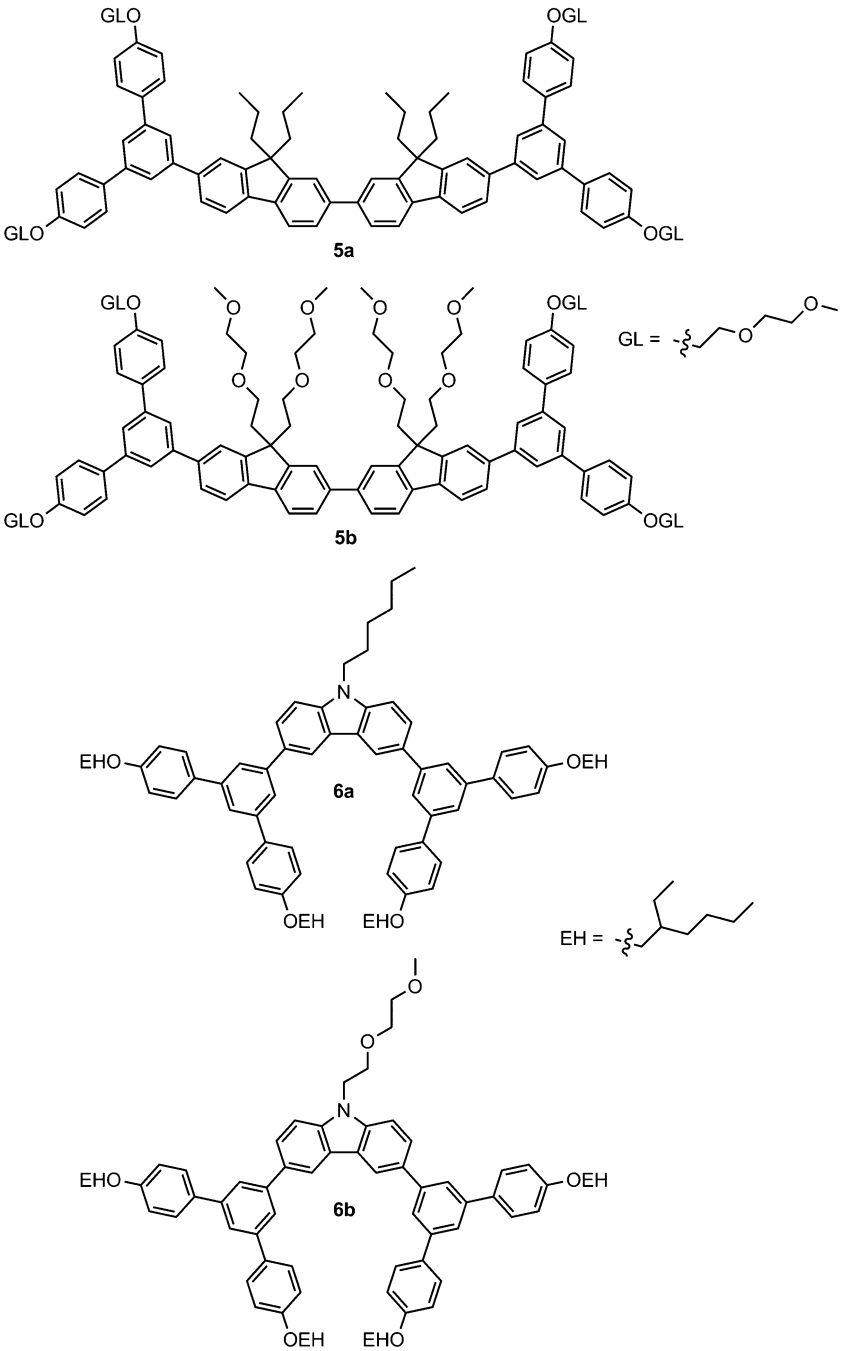

Fig. 1 The chemical structures of the dendrimers used as sensing materials for nitrated analytes.

phases for gas chromatography.[31–33] It was expected that by limiting the chain length to 2-(2-methoxyethoxy)ethyl the solubility of the dendrimers in organic solvents would be maintained. We compare two dendrimer families comprising carbazole or bifluorene cores and first generation biphenyl dendrons (Fig. 1). In each case we compare the effect of changing the solubilising group attached to the core, while keeping the same surface groups [2-ethylhexyloxy or 2-(2-methoxyethoxy)ethyloxy] in each pair. The sensitivities of these dendrimer films towards the nitroaromatic and nitroaliphatic analytes depicted in Fig. 2 were analysed: 2,4-dinitrotoluene (DNT) and 4-nitrotoluene (pNT) are both potential impurities from the manufacture of TNT, and the presence of DNT is commonly used an indicator for the presence of TNT;[16,18,34–38] 1,4-dinitrobenzene (DNB) is a TNT surrogate with a similar saturated vapour concentration and a near-identical reduction potential;[14] nitromethane (NM), whilst not inherently explosive can be mixed with a variety of chemicals to yield explosive compositions;[9,11] and finally, 2,3-dimethyl-2,3-dinitrobutane (DMNB), the volatile tagging agent added to commercially manufactured plastic explosives for detection by trained canines.[10,12]

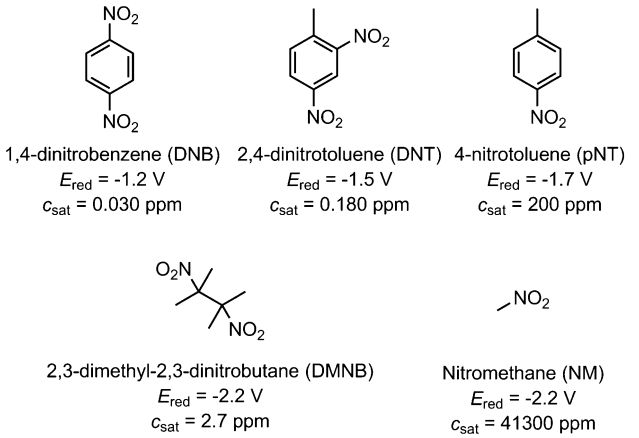

Fig. 2 The structures, first reduction potentials (E_{red} *versus* the ferrocenium/ferrocene couple) and saturated vapour concentrations (c_{sat}) of the nitrated analytes.[13,14,39]

Results and discussion

Dendrimer synthesis

The final steps of the syntheses of the four dendrimers are depicted in Scheme 1 with detailed methods for the preparation of the starting materials in the ESI.† The synthesis of carbazole-based dendrimer **6a** was recently reported by our group and is included in the scheme for completeness.[29] The final step in the convergent synthesis of each dendrimer was a palladium-catalysed Suzuki coupling. The bifluorene-cored dendrimers **5a**/**b** with different solubilising groups on the 9-positions of the fluorene moieties were prepared by reaction of the boronate ester-focussed first generation biphenyl dendrons containing 2-(2-methoxyethoxy)ethyloxy surface groups (**1**) and the dibrominated core precursors (**3a**/**b**). In contrast, for the carbazole-cored dendrimers two 2-ethylhexyloxy-surfaced dendrons (**2**) were attached to **4a**/**b** to give **6a**/**b**. The yield of each dendrimer was greater than 50%. Gel-permeation chromatography showed that the dendrimers were monodisperse and their hydrodynamic radii calculated from their $\bar{M}_v$s were 9.4 Å (**5a**), 9.7 Å (**5b**), 8.4 Å (**6a**) and 8.4 Å (**6b**). Differential scanning calorimetry was used to determine glass transition temperatures (T_gs), which were 60 °C, 27 °C, 30 °C and 26 °C for **5a**, **5b**, **6a** and **6b**, respectively.

Photophysical and electrochemical properties

The absorption and photoluminescence (PL) spectra for solutions and thin films of dendrimers **5a/b** and **6a/b** are shown in Fig. 3. The spectra of the dendrimers with the same core unit were found to be essentially the same, indicating that substitution of the alkyl groups with 2-(2-methoxyethoxy)ethyl groups on the core does not greatly influence the optical properties of the chromophores. In the case of the bifluorene dendrimers the absorption and PL spectra recorded are also consistent with reported bifluorene dendrimers possessing biphenyl-based first generation dendrons and 2-ethylhexyloxy surface groups.[27,40] That is, changing the surface groups on the dendrons does not change the absorption properties of the dendrimers. For the bifluorene-cored dendrimers (**5a**/**b**) the absorption spectra in both dichloromethane solution and thin films display featureless lowest-energy absorptions with a maximum around 350 nm. A second higher-energy peak was also observed at 265 nm, which has a significant contribution from the

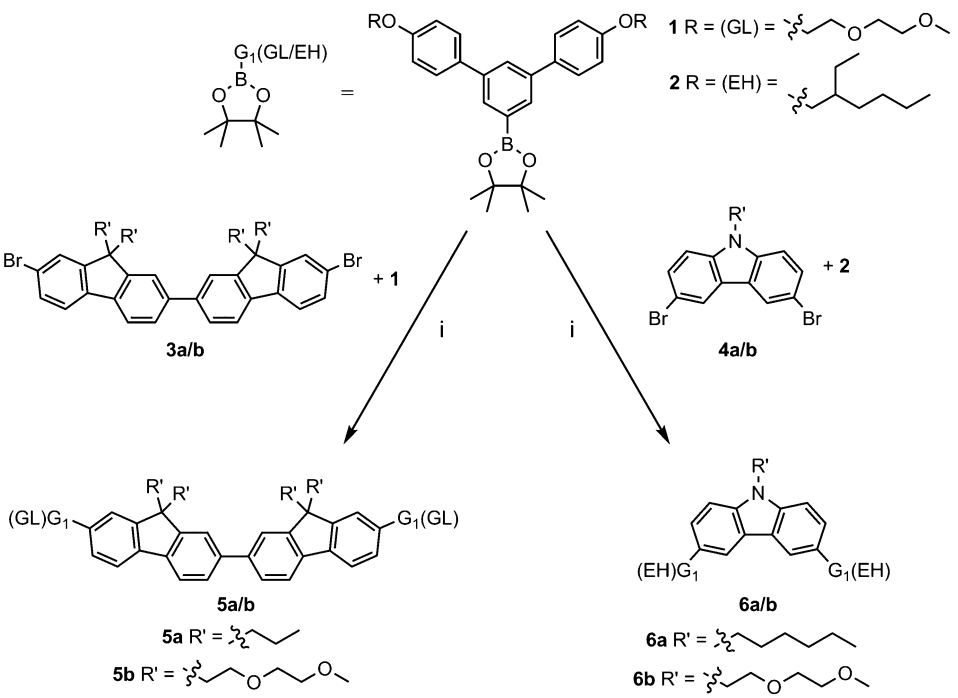

Scheme 1 Synthesis of dendrimers **5a**/**b** and **6a**/**b**. *Conditions and reagents*: (i) $Pd(PPh_3)_4$, PhMe, *tert*-BuOH, aq. K_2CO_3, 100 °C, N_2. Yields: **5a** 53%; **5b** 71%; **6a** 52%; **6b** 59%.

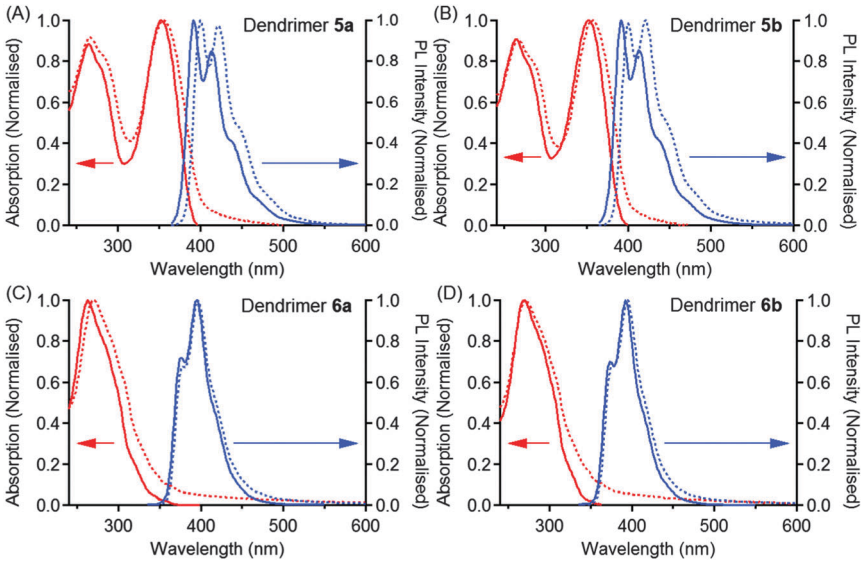

Fig. 3 The normalised absorption and PL spectra for dendrimers **5a** (A), **5b** (B), **6a** (C) and **6b** (D). The solid lines correspond to solution measurements (dichloromethane) and the dashed lines correspond to measurements of thin films spin-coated on glass substrates. For the PL measurements the bifluorene dendrimers **5a/b** were excited at 350 nm and the carbazole dendrimers **6a/b** were excited at 320 nm.

chromophores in the biphenyl dendrons.[41] The solution PL spectra of the bifluorene-cored dendrimers displayed vibronic features with peaks around 392 nm and 413 nm, and shoulders around 435 nm and 465 nm. The thin film absorption and PL spectra only had a small red-shift compared to that in solution. Increased overlap of the dendrimer absorption and PL causes the observed reduction in the PL intensity for the (0–0) vibronic transition relative to the (0–1) transition in the thin film emission profiles. The solution PLQY of dendrimers **5a** and **5b** were found to be 81 ± 1% and 85 ± 1%, respectively, showing that radiative decay of the fluorophore is a highly efficient process. The thin film PLQYs were found to be similar to those in solution with average values of 83 ± 6% and 71 ± 5% for **5a** and **5b**, respectively. These film PLQYs are significantly higher than a similar bifluorene-cored dendrimer that had 2-ethylhexyloxy surface groups and *n*-propyl units on the 9-positions of the fluorenyl moieties (PLQY = 49 ± 5%).[27] The fact that the solution and film PLQYs for the glycolated dendrimers are very similar indicates that the first-generation biphenyl dendrons, surface groups and substituents on the 9-positions of the fluorene units provide sufficient separation of the emissive chromophores to avoid significant aggregation-induced quenching in the solid state.[42] The PL lifetimes of dendrimers **5a/b** were measured at 395 nm in tetrahydrofuran solution and were found to be 0.77 ± 0.01 ns and 0.78 ± 0.01 ns for dendrimers **5a** and **5b**, respectively. Such short PL lifetimes are consistent with previously reported bifluorene dendrimers.[40]

The optical properties of dendrimer **6a** have been reported previously,[29] and those of the glycolated dendrimer **6b** were found to be analogous. The dichloromethane solution absorption spectra of dendrimers **6a** and **6b** had peaks close to the isolated dendron absorption maximum at around 265 nm and displayed a number of shoulders leading to the absorption onset of around 375 nm. The carbazole dendrimer PL spectra displayed emission peaks at 375 nm and 395 nm along with shoulders around 410 nm and 435 nm. The film absorption and PL spectra of the carbazole dendrimers **6a/b** were analogous to their solution counterparts. The carbazole dendrimers **6a** and **6b** were found to have solution PLQYs of 19 ± 1% and 15 ± 1% with thin film PLQYs of 27 ± 6% and 25 ± 6%, respectively. The PL lifetimes of **6a/b** measured at 400 nm in toluene solution were 7.4 ± 0.1 ns and 7.2 ± 0.1 ns, which are an order of magnitude longer than the bifluorene-cored dendrimers and a reason why these and similar dendrimers show enhanced collisional quenching in solution.[29] The higher film PLQYs are consistent with previous reports that 3,6-disubstituted carbazole fluorophores with biphenyl type substituents undergo emission enhancement in the solid state due to deactivation of non-radiative decay pathways by restriction of intramolecular rotations,[43] and that the first-generation dendrons attached directly to the carbazole unit provide enough steric shielding of the emissive fluorophores to prevent significant aggregation quenching of fluorescence in the solid state. Despite having lower PLQYs than the bifluorene dendrimers **5a/b** the emission intensity of the carbazole dendrimers **6a/b** was sufficient for the materials to be used in sensing applications.

We used cyclic voltammetry (CV) in combination with the optical gap derived from Fig. 3 to determine the oxidation and estimate the reduction potentials of the dendrimers in solution. The cyclic voltammograms of the bifluorene dendrimers **5a** and **5b** both had a single chemically reversible oxidation within the measurable potential window (Fig. 4). The $E_{1/2}$s for the first oxidations were 0.9 V *versus* the ferrocenium/ferrocene (Fc^+/Fc) couple for both **5a** and **5b**. The $E_{1/2}$s for the first reductions were too close to the edge of the electrochemical window and so we estimated the reduction potentials by adding the energy of the optical gaps, which were calculated by a standard method.[44]

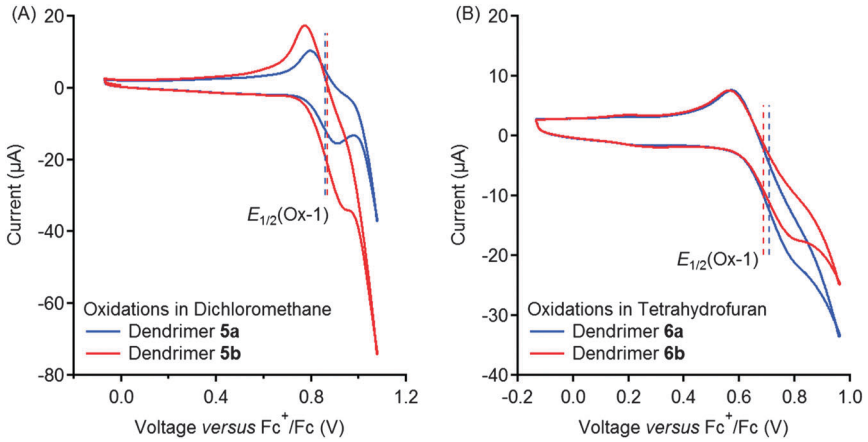

Fig. 4 The oxidation cyclic voltammograms for dendrimers **5a**/**b** (A) and **6a**/**b** (B) in dichloromethane and tetrahydrofuran, respectively. Measurements were referenced to the ferrocenium/ferrocene oxidation $E_{1/2}$ recorded on the day of testing and were performed with a silver/silver nitrate reference electrode in acetonitrile, a glassy carbon working electrode and a platinum counter electrode.

The absorption and PL spectra were normalised in energy by dividing by the photon energy and photon energy cubed, respectively. The rescaled spectra were then normalised to the first absorption and emission features and the intercept between the two curves was taken as the optical energy gap. For both dendrimers **5a** and **5b** the optical energy gap was found to be around 3.3 eV giving estimated reduction potentials of −2.4 V *versus* Fc^+/Fc by subtracting this energy from the observed oxidation potentials.

A chemically reversible oxidation was also observed for the carbazole dendrimers **6a**/**b**. The $E_{1/2}$s of the first oxidations were found to be 0.7 V *versus* Fc^+/Fc for both dendrimers. Voltage sweeps beyond the first oxidation to potentials more positive than 1.0 V *vs.* Fc^+/Fc resulted in a second chemically irreversible oxidation process. The $E_{1/2}$s for the first reductions lay outside of the electrochemical window and so we again estimated the reduction potentials by subtracting the optical gaps of 3.4 eV from the oxidation potentials for dendrimers **6a**/**b**, which gave a value of −2.7 V *versus* Fc^+/Fc.

The reduction potentials *versus* Fc^+/Fc for the higher electron affinity nitroaromatic analytes have been reported to be −1.2 V for DNB, −1.0 V for DNT and −1.7 V for pNT *versus* Fc^+/Fc.[14] The lower electron affinity nitroaliphatic DMNB has a reduction potential of −2.2 V *versus* Fc^+/Fc.[13] The first reduction potential of NM cannot be measured directly by CV as it decomposes to liberate methylhydroxyamine at the electrode surface.[45] However, it is reasonable to expect that the reduction potential for NM would be similar to that of DMNB as both are unconjugated nitroaliphatic molecules. In order for oxidative quenching of the dendrimer fluorescence to occur the difference between the analyte and dendrimer reduction potentials should be greater than the exciton binding energy of the fluorophore, which has been reported to be around 0.5 eV for organic semiconductors.[46] The energy difference between the reduction potentials of the target analytes and those estimated for the dendrimers is $\geq$0.5 eV for most of the dendrimer/analyte combinations suggesting that oxidative quenching of the dendrimer fluorescence was energetically feasible in these cases. The estimated electron affinities of the bifluorene dendrimers **5a**/**b** are only 0.2 eV less than those of the nitroaliphatic analytes and fluorescence quenching might therefore be expected to be weaker or absent. Despite this, quenching was observed when bifluorene dendrimer films were exposed to DMNB and NM and furthermore quenching by DMNB could be enhanced by the choice of core substituent.

Quantitative real time thin film quenching measurements

Film-based fluorescence quenching measurements have generally involved exposure to saturated vapours of the analyte with recovery or cycling achieved by removal of the film from the analyte vapours followed by purging and/or heating of the film to remove the absorbed analyte.[14,15,19,23,35] A problem with this method is that it does not allow accurate determination of the initial quenching response for rapidly diffusing and high electron affinity analytes as substrate immersion takes place prior to the initiation of the PL measurement. The initial rapid adsorption and diffusion of the analytes into fluorescent dendrimer films under steady state conditions has been shown by quartz crystal microbalance with *in situ* PL measurements.[25] Analyte vapour pulses have been reported to be detectable by using a capillary coated with the sensing material and a saturated vapour source.[13,23,47] This procedure, whilst useful for showing a sensors efficacy, defies accurate quantification of film responses towards the analytes as the concentration entering the capillary is unknown. It is unlikely that either saturated analyte vapours or sustained steady state analyte concentrations would be present for sensing in the field and to this end we have developed a method to quantify responses to sub-saturated analyte vapour pulses in real time for thin films. Thin films of the dendrimers were spin-coated onto fused silica substrates from 10 mg cm^{-3} solutions in toluene at 2000 rpm. Under these conditions the resulting films were found to be 40–55 nm thick. The substrates were clamped in a custom made sample chamber in a fluorometer and a constant flow of nitrogen was passed over the film *via* a mass flow controller. Syringes were charged with analyte

and plugged with sufficient cotton wool to prevent injection of the solids. The syringes were primed with nitrogen to eliminate additional quenching by oxygen and stoppered to allow the atmosphere to saturate with analyte vapour for at least 16 hours at ambient temperature prior to analyte injection. Known volumes of analyte-saturated nitrogen were manually injected into the carrier gas flow over a one second period to introduce pulses of analyte into the nitrogen stream. The PL of the films at 400 nm was monitored before, during, and after exposure. The maximum concentration of analyte vapour that could be introduced into the cell was limited by the saturated vapour concentrations of the analytes (Fig. 1).[13,14,39] The analyte concentrations could be varied by either altering the carrier gas flow rate or by injecting different volumes of saturated analyte vapour.

Initial experiments with bifluorene dendrimer **5a** revealed that no responses occurred for the lower electron affinity analyte DMNB with a carrier gas flow of 4000 cm^3 min^{-1}, even when injecting up to 24 cm^3 s^{-1} of saturated analyte vapour (exposure concentration = 0.58 ± 0.11 ppm). However, a measurable reduction in the fluorescence was seen for the higher electron affinity analytes and the highly volatile NM at this flow rate. Reducing the carrier gas flow to 1000 cm^3 min^{-1} decreased the dilution of the analyte vapour and enabled the presence of DMNB vapour to be detected. Thus a 4000 cm^3 min^{-1} carrier gas flow rate was used for the higher electron affinity analytes DNB, DNT and pNT, and a 1000 cm^3 min^{-1} flow rate was used with the lower electron affinity analytes DMNB and NM. It should be noted that varying the carrier gas flow rate should affect the rate of film fluorescence recovery and hence we do not directly compare recovery for measurements at different flow rates.

All of the measurements were performed at ambient temperature, repeated on separate dendrimer films and each film was used for multiple measurements. To confirm the reproducibility of the results the analytes injected during a given quenching experiment were varied along with the concentrations injected. By randomising the order of analyte injections between runs the influence of the film history on responsiveness could be investigated. The carrier flow rate was not altered within a given measurement. Representative thin film quenching traces for each of the dendrimers and analytes are given in Fig. 5. The differences in the shape of the PL baseline signal are due to the observed time slices occurring at different points in the hour-long monitoring period. That is, the films typically had a 'burn in' period that showed faster initial PL degradation than at later times during the scan. However, it is important to note that the rate of background PL decay was very much less than the changes in PL observed on introduction of the analyte and were ignored in the analysis.

Rapid quenching was observed after injection of the analytes into the carrier gas flow with responses reaching a maximum within 1–2 s after injection. Carrier gas volumes equivalent to the internal volume of the sample chamber (~40 cm^3) flow every 1–3 s at the flow rates used and we have assumed that the analyte pulses were rapidly purged from the cell after this time. There are some clear differences between the dendrimers in their behaviour towards the analytes, the most prominent being that the fluorescence of the glycolated dendrimers **5b** and **6b** was more strongly quenched than that of their alkylated counterparts **5a** and **6a** by the nitroaliphatic tagging agent DMNB. The ability of a sensing element to recover after a quenching interaction is not a ubiquitous property of all sensing fluorophores with some requiring thermal or chemical reactivation after exposure to enable further sensing.[19,28,30] Therefore, the recovery of the majority of the film PL is an important result for real time sensing. It is interesting to note that the initial rates of recovery after injection were consistent with the relative volatilities of the analytes. For example, slow recovery was observed after injection of the lower volatility analytes DNB and DNT, despite using the higher carrier gas flow rate of 4000 cm^3 min^{-1}. The fact that the PL does not fully recover suggests that some analyte remains trapped within the film.[30] It is also worthy of note that DMNB was the only analyte that demonstrated a rapid and complete recovery of the film PL in all cases.

The Stern–Volmer equation (1) is commonly used to characterise solution-based quenching interactions,[44]

$$\frac{F_0}{F} = 1 + K[\mathrm{Q}] \quad (1)$$

where [Q] is the quencher (analyte) concentration and K is a constant that serves as a measure of the strength of the quenching interactions occurring – the larger the value of K, the stronger the interaction. In order to quantify the thin film quenching efficiencies we undertook a 'Stern–Volmer' like analysis whereby the PL intensity immediately prior to analyte exposure (F_0) was divided by the PL at the base of the quenching trough (F) and the values of F_0/F plotted against the injected analyte concentrations (Fig. 6). Taking the value of F_0 from just prior to an injection renormalised each response to account for any analyte trapped in the film from previous injections or loss of initial PL intensity due to photodegradation. The analysis is valid if a steady-state excited fluorophore population is established under constant illumination and if the quenching interactions are rapid over the one second exposure time.[44] Within the error of the measurements linear correlations of F_0/F with analyte concentration were observed for each of the dendrimer films. The data collected were consistent between multiple quenching runs regardless of the order of analyte injection and, as such, the exposure history of a film appeared to have little influence on the magnitude of subsequent quenching interactions. Such behaviour is advantageous for long-term use of the sensing element in a portable detection system for continuous monitoring. All the analytes except DMNB showed a first order dependence on analyte concentration with intercepts close to the theoretical value of 1.0 for a standard Stern–Volmer analysis. For DMNB the intercepts were <1.0 suggesting that additional physical factors hindering quenching are leading to higher threshold concentrations for a response to be observed.

The quenching constants K determined from Fig. 6 and the corresponding detection limit concentrations at F_0/F = 1.01 (*i.e.*, the concentration corresponding to a 1% change in fluorescence) are given in Fig. 7 (values are tabulated in the ESI†). In general the bifluorene dendrimers **5a**/**b** were found to be more sensitive to the nitroaromatics with DNT, DNB

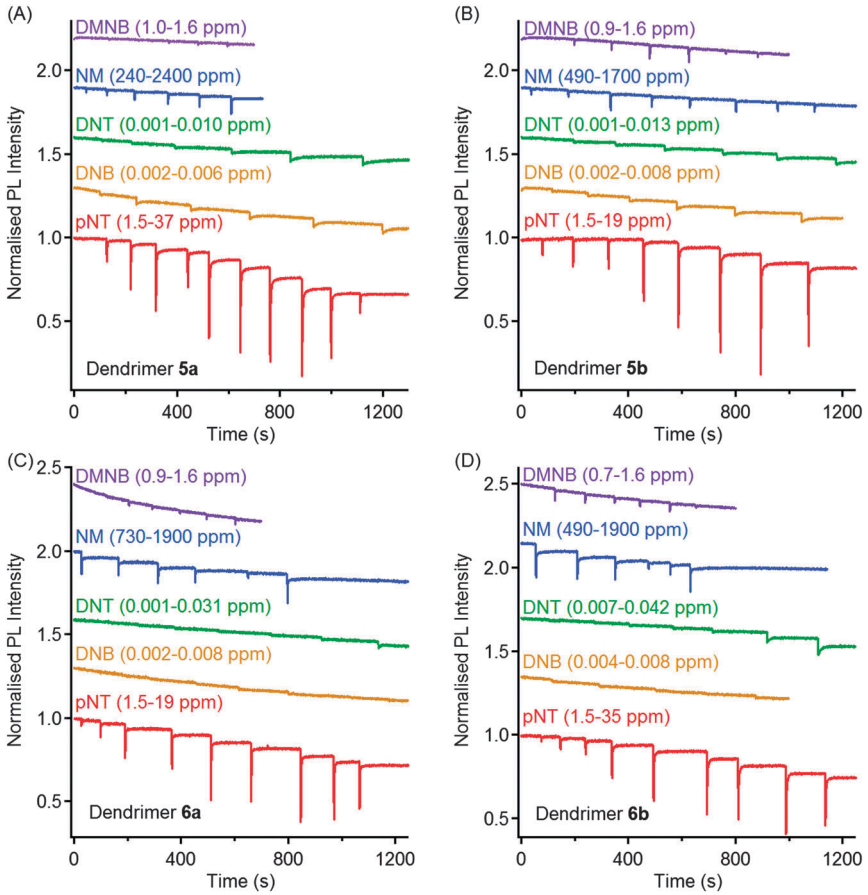

Fig. 5 Thin film quenching traces for the bifluorene dendrimers **5a** (A) and **5b** (B) and the carbazole dendrimers **6a** (C) and **6b** (D). All plots are on the same PL and time scales and the traces are offset for clarity. Numbers in parentheses indicate the range of vapour concentrations injected into the cell. The order of injected analyte concentrations was randomised and in each case the magnitude of the decrease in PL increases with the amount of analyte injected.

and pNT having larger quenching constants and thereby lower detection limits for these analytes than the carbazole dendrimers **6a**/**b** (note the log scale on the *Y*-axes visually compresses these differences). The detection limits of the bifluorene dendrimers for DNB of $(0.95 \pm 0.19) \times 10^{-3}$ ppm (**5a**) and $(1.21 \pm 0.24) \times 10^{-3}$ ppm (**5b**) were around 4% of the saturated analyte vapour concentration. Similarly, the detection limit concentrations of the bifluorene dendrimers of $(1.82 \pm 0.36) \times 10^{-3}$ ppm (**5a**) and $(2.35 \pm 0.47) \times 10^{-3}$ ppm (**5b**) for DNT were around 1% of the saturated concentration showing the strong sensitivity of these dendrimers towards traces of the high electron affinity nitroaromatics. The sensitivity of the carbazole dendrimers **6a**/**b** was around 4–5 times less than that of the bifluorene dendrimers, with detection limits around 4% of the saturated concentration of DNT and 18% of the saturated concentration of DNB. The quenching constants for the higher volatility and lower electron affinity analytes NM and pNT were lower than for DNT and DNB. However, all of the dendrimers gave detection limit concentrations that were $<1\%$ of the saturated vapour concentrations of NM and pNT, showing that these volatile analytes can be detected at high dilution.

The polarity of the core solubilising groups was found to have a subtle influence on the dendrimer sensitivities towards DNT, DNB, pNT and NM. Dendrimers **5a** and **6b** with a mix of oligo(ethylene oxide) and alkyl solubilising groups on the core and the dendrons showed slightly greater sensitivities towards DNT, DNB and NM, whilst dendrimers **5b** and **6a** with all polar or all non-polar solubilising groups showed greater sensitivity towards pNT. This suggests that the interplay between the polarity of the substituents on the core and dendrons exerts some influence on the degree of quenching by the different analytes in the thin films. However, as a result of having oligo(ethylene oxide) chains on the core units the sensitivity of DMNB detection is significantly increased. That is, both dendrimers **5b** and **6b** showed enhanced sensitivity towards the nitroaliphatic tagging agent when compared with their alkylated counterparts. The most significant enhancement in quenching constant was a factor of 5 increase in sensitivity when the four *n*-propyl chains of **5a** were exchanged for 2-(2-methoxyethoxy)ethylchains on the bifluorene core to give **5b**. The corresponding sensitivity enhancement when exchanging the single *n*-hexyl chain of **6a** for a 2-(2-methoxyethoxy)ethyl chain on the carbazole core of dendrimer **6b** was only a factor of 2. This suggests that the influence of the oligo(ethylene oxide) chains is additive, with greater sensitivity enhancement observed for the dendrimers with more groups attached to the core.

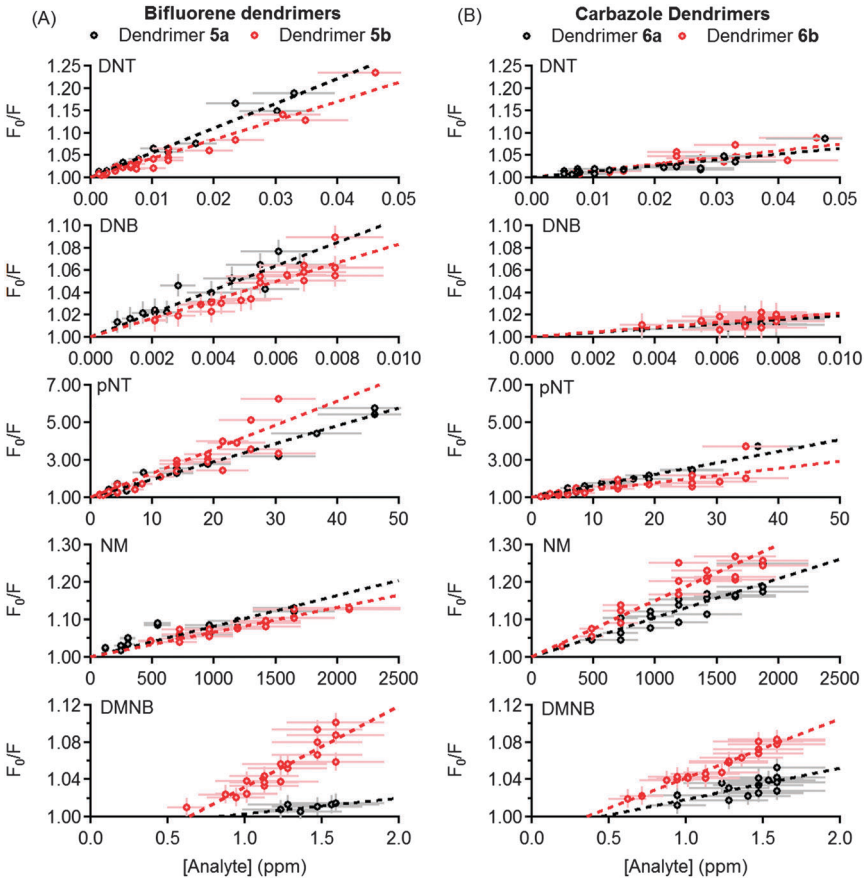

Fig. 6 F_0/F *versus* analyte concentration plots for thin films of dendrimers **5a/b** (A) and **6a/b** (B) using nitrogen carrier gas flows of 4000 cm^3 min^{-1} for DNT, DNB and pNT and 1000 cm^3 min^{-1} for NM and DMNB. Individual points indicate recorded experimental data and a description of the error analysis is given in the Experimental details. In both cases black indicates alkyl core substituents, red indicates glycol core substituents and dashed lines indicate straight line fits to the data.

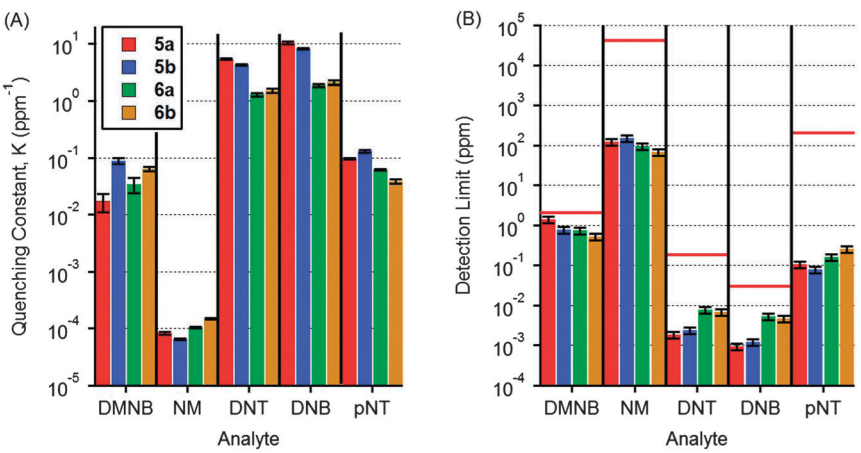

Fig. 7 The quenching constants K (A) and detection limit concentrations (B) for the analytes tested. The quenching constants and associated errors were determined from the gradient of the straight line fits in Fig. 6. The detection limit concentrations represent the minimum analyte concentration that produces a 1% (F_0/F = 1.01) fluorescence quenching response over a one second exposure. Horizontal red lines in (B) indicate the saturated vapour concentration of each analyte given in Fig. 2.

Conclusions

In summary, we have developed bifluorene- and carbazole-cored dendrimers with first generation biphenyl-based dendrons for explosive sensing. Reversible fluorescence quenching interactions were observed upon exposure of dendrimer thin films to sub-saturation vapour concentrations of nitroaromatic and

nitroaliphatic vapours, showing their ability to detect traces of these target analytes. The quenching responses were quantified as a function of analyte concentration using a Stern–Volmer-like analysis akin to that used for solution-based quenching analysis. The inclusion of 2-(2-methoxyethoxy)ethyl substituents on both the bifluorene and the carbazole units was found to increase the sensitivity towards the nitroaliphatic tagging agent DMNB. Detection of this nitroaliphatic tagging agent by oxidative fluorescence quenching is normally challenging, and the ability to molecularly engineer enhanced sensitivity by simple chemical substitutions is a strength of dendritic sensing materials. The quenching interactions were also independent of film exposure history under continuous illumination, making these molecules strong candidates for deployment in field portable vapour sensors for continuous monitoring of nitroaliphatic and nitroaromatic vapours.

Experimental details

General experimental methods and synthesis of organic compounds

Unless otherwise stated, chemicals were obtained from commercial sources and used as received. Solvents were distilled by rotary evaporation under reduced pressure before use. Anhydrous tetrahydrofuran used for reactions was dried over sodium benzophenone and distilled immediately prior to use.

Thin layer chromatography was performed on Aldrich aluminium plates coated with silica gel 60 P_{254}. Column chromatography was performed with Merck silica gel (0.063–0.200 mm). Chromatotron separations were performed using plates of Silica Gel 60 PF_{254} containing gypsum on a T-squared Technology Chromatotron 7924T. When solvent mixtures were used as eluent the proportions are given by volume. Kügelrohr distillations were performed using a Büchi B-585 Kügelrohr.

^{1}H and ^{13}C NMR spectra were recorded on Bruker AV300, AV400 or AV500 spectrometers. Chemical shifts are reported in parts per million (ppm) and are referenced to the residual solvent peak [$\delta_H(CHCl_3)$ = 7.26, $\delta_C(CDCl_3)$ = 77.0]. Coupling constants, J, are reported in Hertz (Hz) to the nearest 0.5 Hz. Peak multiplicities are labelled in the following manner: singlet (s), doublet (d), triplet (t), multiplet (m) and broad (br); aromatic peak identities are abbreviated as Ar (aryl), Ph (phenyl), Fl (fluorenyl) and Cbz (carbazolyl).

MALDI-TOF mass spectra were recorded on an Applied Biosystems Voyager MALDI-TOF mass spectrometer using 1,8,9-anthracenetriol as the matrix. ESI mass spectra were recorded on a Bruker HCT 3D Ion Trap using methanol/dichloromethane as the solvent. ESI mass spectra and elemental microanalysis were performed by the respective mass spectrometry and microanalysis facilities at the School of Chemistry and Molecular Biosciences, UQ.

UV-visible absorption spectra were measured on a Varian Cary 5000 UV-Vis-NIR spectrophotometer in spectrophotometric grade solvents. λ_{max} values are quoted in nm and shoulders denoted by sh.

Gel permeation chromatography was performed on a Polymer Laboratories PL GPC 50 using PLgel 3 μm mixed-E columns (2 × 300 mm lengths, 7.5 mm diameter) from Polymer Laboratories calibrated against polystyrene narrow standards [$\bar{M}_p$ = (162–3.8) × 10^4] in tetrahydrofuran containing 0.01% toluene as a flow marker. The eluent was degassed with helium and pumped at a rate of 0.5 cm^3 min^{-1} at 39.3 °C. UV absorption at 256 nm was used to detect the eluting species.

Glass transition temperatures (T_g) were recorded on a Perkin Elmer Diamond DSC Differential Scanning Calorimeter within the temperature range −150 to 200 °C. Scan rates of between 20 and 100 °C min^{-1} were used and the heating and cooling rates were identical during each scan. Heating/cooling rates are quoted with reported T_gs. Decomposition temperatures ($T_{5\%\ dec}$) are quoted for 5% weight loss and were recorded on a Perkin Elmer STA 6000 Simultaneous Thermal Analyser. Samples were heated from 30–800 °C at 10 °C min^{-1} for $T_{5\%\ dec}$ determination. Melting points were measured using a Büchi Melting Point B-545 and are corrected.

Cyclic Voltammetry (CV) was recorded on a BASi EpsilonEC. The potentials quoted are referenced to the ferrocenium/ferrocene (Fc^+/Fc) couple measured on the day of testing. A silver/silver nitrate reference electrode in acetonitrile, a platinum counter electrode and a glassy carbon working electrode were used. Scan rates between 100 and 1000 mV s^{-1} were used for the CV measurements. The measured potentials are denoted $E_{1/2}$ (redox process, solvent, working electrode). For electrochemical measurements dichloromethane was distilled over calcium hydride and tetrahydrofuran was distilled over sodium/benzophenone and then distilled over lithium aluminium hydride.

Thin films were formed by spin-coating 10 mg cm^{-3} dendrimer solutions in spectrophotometric grade toluene using a Speciality Coating Systems (SCS) G3-8 Spincoater. Glass and fused silica substrates were cleaned by ultrasonication in acetone, 2-propanol and the deposition solvent prior to film spinning. Surface contact profilometry to determine film thickness was performed on a Veeco Dektak 150.

2-(3,5-Bis{4-[2-(2-methoxyethoxy)ethoxy]phenyl}phenyl)-4,4,5,5-tetramethyl-1,3,2-dioxaborolane (1). **9** (0.424 g, 0.777 mmol) was dissolved in anhydrous tetrahydrofuran (2.5 cm^3) under argon and the resulting solution was chilled in a dry ice/acetone bath. A solution of *n*-butyl lithium in hexanes (1.6 M, 2.0 cm^3) was added and the mixture was stirred whilst chilled for a further 15 min. 2-Iso-propoxy-4,4,5,5-tetramethyl-1,3,2-dioxaborolane (0.70 cm^3, 3.4 mmol) was added and the mixture was stirred in the dry ice/acetone bath for a further 10 min. The mixture was allowed to warm to room temperature and was stirred for 3 d. The mixture was quenched with water (20 cm^3) and diluted with diethyl ether (20 cm^3). The layers were separated and the aqueous layer was extracted with diethyl ether (3 × 5 cm^3). The combined organics were washed with water (2 × 5 cm^3) and brine (5 cm^3). The organics were dried over anhydrous magnesium sulfate and filtered. The magnesium sulfate was washed with additional diethyl ether and the filtered organics combined before the volatiles were removed *in vacuo*. The crude residue was separated in two stages: firstly residual boronated

impurities were removed by short-path distillation using a Kügelrohr distillation apparatus at 0.4 mbar and 100 °C and finally debrominated by-products in the residue were crystallised from diethyl ether at 0 °C and removed from the product by filtration. Removal of the volatiles from the filtrate *in vacuo* yielded **1** as an off-white solid (0.382 g, 83%), mp = 79–84 °C. Found C, 68.8; H, 7.8; $C_{34}H_{45}BrO_8$ requires C, 68.9; H, 7.7. λ_{max} (CH_2Cl_2/nm): 267 (log ε/dm^3 mol^{-1} cm^{-1} 4.60). δ_H (300 MHz, $CDCl_3$): 1.37 (12H, br s, ArB[OC(CH_3)$_2$]$_2$), 3.40 (6H, s, ArOC_2H_4OC_2H_4OCH_3), 3.58–3.61 (4H, m, ArOC_2H_4OCH_2CH_2OMe), 3.73–3.76 (4H, m, ArOC_2H_4OCH_2-CH_2OMe), 3.87–3.91 (4H, m, ArOCH_2CH_2OC_2H_4OMe), 4.18–4.21 (4H, m, ArOCH_2CH_2OC_2H_4OMe), 6.99 and 7.60 (8H, AA′BB′, surface PhH), 7.81 (1H, dd, J = 2.0 Hz, J = 2.0 Hz, branching PhH), 7.94 (2H, d, J = 2.0 Hz, branching PhH). δ_C (125 MHz, $CDCl_3$): 24.8, 59.1, 67.4, 69.8, 70.7, 71.9, 83.9, 114.8, 128.1, 128.3, 131.5, 133.8, 140.6, 158.3. *m*/*z* [ESI] anal. calcd for $C_{34}H_{45}BO_8$: 591.3 (25%), 592.3 (100%), 593.3 (37%). Found 614.3 (17%, M + Na^+), 615.3 (100%, M + Na^+) and 616.3 (28%, M + Na^+). Note – the product isolated was observed to degrade by hydrolysis if exposed to wet solvents or atmospheric moisture. The data quoted is for freshly isolated **1** but over time the ^{1}H NMR peak at 1.37 ppm was found to decrease in intensity and additional aromatic resonances in the range 7.4–7.6 ppm were observed.

7,7′-Dibromo-9,9,9′,9′-tetrakis[2-(2-methoxyethoxy)ethyl]-2,2′-bifluorene (3b). 9,9,9′,9′-Tetrakis[2-(2-methoxyethoxy)ethyl]-2,2′-bifluorene **11b** (1.12 g, 1.52 mmol) was dissolved in chloroform (15 cm^3) and a small iodine crystal was added. Light was excluded and a solution of bromine (0.583 g, 3.65 mmol) in chloroform (10 cm^3) was added. The mixture was stirred at room temperature for 3 d before it was quenched with aqueous sodium metabisulfite (0.5 M, 30 cm^3). After the loss of all bromine/iodine colouration the mixture was diluted with chloroform (30 cm^3) and water (20 cm^3) and the layers were separated. The aqueous layer was extracted with chloroform (3 × 10 cm^3) and the combined organics were washed with water (2 × 30 cm^3) and brine (2 × 30 cm^3). The organics were dried over anhydrous magnesium sulfate and filtered. The magnesium sulfate was washed with additional chloroform and the filtered organics combined before the volatiles were removed *in vacuo*. The crude residue was purified by column chromatography over silica using ethyl acetate as eluent yielding **3b** as a yellow oil that slowly crystallised into a pale yellow solid (0.943 g, 69%), mp = 88–89 °C. Found C, 61.5; H, 6.2; $C_{46}H_{56}Br_2O_8$ requires C, 61.6; H, 6.3. λ_{max} (CH_2Cl_2/nm): 268sh (log ε/dm^3 mol^{-1} cm^{-1} 3.72), 280sh (3.97), 310sh (4.53) and 335 (4.81). δ_H (500 MHz, $CDCl_3$): 2.42–2.52 (8H, m, FlC$H_2$$CH_2$O-$C_2H_4$OMe), 2.76–2.88 (8H, m, FlCH_2CH_2OC_2H_4OMe), 3.17–3.26 (8H, m, FlC_2H_4OCH_2CH_2OMe), 3.27 (12H, s, FlC_2H_4OC_2H_4-OCH_3), 3.31 (8H, t, J = 4.5 Hz, FlC_2H_4OCH_2CH_2OMe), 7.49 (2H, dd, J = 8.0 Hz and 1.5 Hz, FlH), 7.58 (2H, d, J = 8.0 Hz, FlH), 7.59 (2H, d, J = 1.5 Hz, FlH), 7.63 (2H, dd, J = 7.5 Hz and 1.5 Hz, FlH), 7.65 (2H, br s, FlH), 7.73 (2H, d, J = 7.5 Hz, FlH). δ_C (125 MHz, $CDCl_3$): 39.7, 51.7, 59.0, 66.9, 69.9, 71.7, 120.2, 121.2, 121.3, 121.6, 126.7, 126.8, 130.5, 138.8, 139.1, 140.7, 149.4, 151.4. *m*/*z* [MALDI-TOF] anal. calcd 894.2 (47%), 895.2 (25%), 896.2 (100%), 897.2 (50%), 898.2 (58%), 899.2 (24%), 900.2 (8%). Found 894.5 (45%), 895.5 (21%), 896.5 (100%), 897.5 (44%), 898.5 (61%), 899.5 (18%).

3,6-Dibromo-9-[2-(2-methoxyethoxy)ethyl]carbazole (4b). 3,6-Dibromocarbazole[48] (1.50 g, 4.62 mmol) was dissolved in dimethylsulfoxide (5.0 cm^3) and aqueous potassium hydroxide (50% w/w, 5.0 cm^3) was added. 1-Bromo-2-(2-methoxyethoxy)ethane (0.93 cm^3, 6.9 mmol) was added to the mixture, which was stirred at room temperature for 4 h. The mixture was diluted with diethyl ether (150 cm^3), ethyl acetate (50 cm^3) and water (100 cm^3), and the layers were separated. The aqueous layer was extracted with ethyl acetate (2 × 50 cm^3) and the combined organics were washed with water (2 × 50 cm^3) and brine (50 cm^3). The organics were dried over anhydrous magnesium sulfate and decanted. The magnesium sulfate was washed with additional ethyl acetate and the decanted organics combined before the volatiles were removed *in vacuo*. The crude residue was separated by column chromatography over silica using an ethyl acetate/*n*-hexane mixture (2 : 3) as eluent to give **4b** as a white powder (1.78 g, 90%), mp = 115–116 °C. Found C, 47.7; H, 4.1; N, 3.2; $C_{17}H_{17}NO_2Br_2$ requires C, 47.8; H, 4.0; N, 3.3. λ_{max} (CH_2Cl_2/nm): 236 (log ε/dm^3 mol^{-1} cm^{-1} 5.35), 242 (5.34), 251 (5.13), 273 (5.12), 292sh (4.62) 298sh (4.71), 304 (4.92), 334sh (4.03), 345 (4.21), 345sh (4.16) and 360 (4.21). δ_H (500 MHz, $CDCl_3$): 3.29 (3H, s, N(C_2H_4)O(C_2H_4)OCH_3), 3.38–3.40 (2H, m, N(C_2H_4)OCH_2CH_2OCH_3), 3.47–3.49 (2H, m, N(C_2H_4)OCH_2CH_2OCH_3), 3.83 (2H, t, J = 6.0 Hz, NCH_2CH_2O-(C_2H_4)OCH_3), 4.44 (2H, t, J = 6.0 Hz, NCH_2CH_2O(C_2H_4)OCH_3), 7.33 (2H, d, J = 8.5 Hz, CbzH), 7.54 (2H, dd, J = 8.5 Hz and 2.0 Hz, CbzH), 8.12 (2H, d, J = 2.0 Hz, CbzH). δ_C (125 MHz, $CDCl_3$): 43.5, 59.0, 69.3, 70.9, 71.9, 110.7, 112.2, 123.1, 123.5, 129.0, 139.5. *m*/*z* [ESI] anal. calcd for $C_{17}H_{17}NO_2Br$ 425.0 (51%), 427.0 (100%), 429.0 (49%). Found 426.0 (18%, M + H^+), 428.0 (35%, M + H^+), 430.0 (16%, M + H^+), 447.9 (53%, M + Na^+), 449.9 (100%, M + Na^+), 451.9 (48%, M + Na^+), 463.9 (43%, M + K^+), 465.9 (73%, M + K^+), 467.9 (41%, M + K^+).

7,7′-Bis(3,5-bis{4-[2-(2-methoxyethoxy)ethoxy]phenyl}phenyl)-9,9,9′,9′-tetra-*n*-propyl-2,2′-bifluorene (5a). **3a**[49] (0.500 g, 0.762 mmol) and **1** (1.13 g, 1.90 mmol) were dissolved in toluene (40 cm^3). Aqueous potassium carbonate (2.0 M, 13 cm^3) and *tert*-butanol (13 cm^3) were added and the mixture was deoxygenated by sparging with nitrogen for 40 min. Tetrakis(triphenylphosphine)palladium(0) (0.088 g, 0.076 mmol) was added and the mixture was deoxygenated by sparging with nitrogen for 30 min. The mixture was stirred at 100 °C under nitrogen for 3 d before it was allowed to cool to room temperature. The mixture was diluted with toluene (60 cm^3) and water (30 cm^3) and the layers were separated. The aqueous layer was extracted with toluene (6 × 20 cm^3) and the combined organics were washed with water (2 × 20 cm^3) and brine (20 cm^3). The organics were dried over anhydrous magnesium sulfate and filtered. The magnesium sulfate was washed with additional toluene and the filtered organics combined before the volatiles were removed *in vacuo*. The crude residue was initially separated by column chromatography over silica using ethyl acetate/*n*-hexane/methanol mixtures (1 : 1 : 0–19 : 0 : 1) as eluent. Fractions containing **5a** were combined and purified by chromatotron chromatography in three stages: firstly using ethyl acetate/*n*-hexane mixtures (1 : 1–3 : 1) as eluent; secondly using a chloroform/ethanol

mixture (99 : 1) as eluent and finally using dichloromethane/methanol mixtures (1 : 0–49 : 1) as eluent. This sequence of purifications yielded **5a** as a colourless glassy solid (0.579 g, 53%). Found C, 79.4; H, 7.8; $C_{94}H_{106}O_{12}$ requires C, 79.1; H, 7.5. λ_{max} (CH_2Cl_2/nm): 253sh ($\log \varepsilon$/dm^3 mol^{-1} cm^{-1} 4.80), 265 (4.88), 275sh (4.83) and 353 (4.93). δ_H (500 MHz, $CDCl_3$): 0.73 (12H, t, J = 7.0 Hz, FlCH$_2$CH$_2$CH_3), 0.77–0.87 (8H, m, FlCH$_2$CH_2CH$_3$), 2.07–2.14 (8H, m, FlCH_2CH$_2$CH$_3$), 3.42 (12H, s, ArOC$_2$H$_4$OC$_2$H$_4$OCH_3), 3.60–3.62 (8H, m, ArOC$_2$H$_4$OCH$_2$CH_2OMe), 3.75–3.77 (8H, m, ArOC$_2$H$_4$OCH_2CH$_2$OMe), 3.92 (8H, t, J = 5.0 Hz, ArOCH$_2$CH_2OC$_2$H$_4$OMe), 4.23 (8H, t, J = 5.0 Hz, ArOCH_2CH$_2$OC$_2$H$_4$OMe), 7.06 (8H, 1/2AA′BB′, surface PhH), 7.65–7.72 (18H, m, overlapping branching PhH, surface PhH and FlH), 7.77 (4H, d, J = 1.5 Hz, branching PhH), 7.83 (4H, br dd, J = 8.0 Hz, J = 2.0 Hz, FlH). δ_C (125 MHz, $CDCl_3$): 14.6, 17.3, 42.8, 55.6, 59.1, 67.5, 69.8, 70.8, 72.0, 115.0, 120.0, 121.4, 121.7, 124.3, 124.4, 126.2, 126.3, 128.4, 134.0, 139.9, 140.17, 140.25, 140.5, 141.9, 142.7, 151.77, 151.79, 158.5. m/z [MALDI-TOF] anal. calcd 1426.8 (95%), 1427.8 (100%), 1428.8 (54%), 1429.8 (20%), 1430.8 (6%). Found 1426.9 (98%), 1427.9 (100%), 1428.8 (53%), 1429.9 (36%), 1430.9 (10%). PLQY (solution) = 0.81 ± 0.01, PLQY (film) = 0.83 ± 0.06. T_g (100 °C min^{-1}) = 60 ± 1 °C (no melting transitions observed below 200 °C). $T_{5\%\ dec}$ = 383 °C. $E_{1/2}$ (Ox-1, CH_2Cl_2, Glassy C) = 0.86 V. GPC: $\bar{M}_n$ = 1954, $\bar{M}_w$ = 1962, $\bar{M}_v$ = 1961.

7,7′-Bis(3,5-bis{4-[2-(2-methoxyethoxy)ethoxy]phenyl}phenyl)-9,9,9′,9′-tetrakis[2-(2-methoxyethoxy)ethyl]-2,2′-bifluorene (5b). **3b** (0.074 g, 0.083 mmol) and **1** (0.122 g, 0.207 mmol) were dissolved in toluene (5.0 cm^3). Aqueous potassium carbonate (2.0 M, 1.5 cm^3) and *tert*-butanol (1.5 cm^3) were added and the mixture was deoxygenated by sparging with nitrogen for 30 min. Tetrakis(triphenylphosphine)palladium(0) (0.010 g, 0.009 mmol) was added and the mixture was deoxygenated by sparging with nitrogen for 20 min. The mixture was stirred at 100 °C under nitrogen for 2 d before it was allowed to cool to room temperature. The mixture was diluted with ethyl acetate (20 cm^3) and water (15 cm^3) and the layers were separated. The aqueous layer was extracted with ethyl acetate (3 × 5 cm^3) and the combined organic layers were washed with water (2 × 5 cm^3) and brine (5 cm^3). The organics were dried over anhydrous magnesium sulfate and filtered. The magnesium sulfate was washed with additional ethyl acetate and the filtered organics combined before the volatiles were removed *in vacuo*. The crude residue was initially separated by column chromatography over silica using *n*-hexane/ethyl acetate/methanol mixtures (1 : 9 : 0–0 : 19 : 1) as eluent. Fractions containing **5b** were combined and purified by chromatotron chromatography in two stages: firstly using ethyl acetate/methanol mixtures (1 : 0–97 : 3) as eluent and finally using chloroform/ethanol/methanol mixtures (99 : 1 : 0–98 : 1 : 1) as eluent. This sequence of purifications yielded **5b** as a colourless gum (0.098 g, 71%). Found C, 73.2; H, 7.3; $C_{102}H_{122}O_{20}$ requires C, 73.4; H, 7.4. λ_{max} (CH_2Cl_2/nm): 254sh ($\log \varepsilon$/dm^3 mol^{-1} cm^{-1} 4.77), 265 (4.83), 278sh (4.77) and 352 (4.87). δ_H (500 MHz, $CDCl_3$): 2.57 (8H, br t, J = 7.5 Hz, FlCH_2CH$_2$OC$_2$H$_4$OMe), 2.86–2.94 (8H, m, FlCH$_2$CH_2OC$_2$H$_4$OMe), 3.21–3.27 (20H, m, overlapping FlC$_2$H$_4$OCH_2CH$_2$OMe and FlC$_2$H$_4$OC$_2$H$_4$OCH_3), 3.31 (8H, t, J = 4.5 Hz, FlC$_2$H$_4$OCH$_2$CH_2OMe), 3.42 (12H, s, ArOC$_2$H$_4$OC$_2$H$_4$OCH_3), 3.60–3.62 (8H, m, ArOC$_2$H$_4$OCH$_2$CH$_2$OMe), 3.75–3.77 (8H, m, ArOC$_2$H$_4$OCH_2CH$_2$OMe), 3.91–3.93 (8H, m, ArOCH$_2$CH_2OC$_2$H$_4$OMe), 4.22–4.24 (8H, m, ArOCH_2CH$_2$OC$_2$H$_4$OMe), 7.06 and 7.67 (16H, AA′BB′, surface PhH), 7.70–7.74 (8H, m, overlapping FlH), 7.77 (2H, br d, branching PhH), 7.78 (4H, d, J = 1.5 Hz, branching PhH), 7.82 (4H, dd, J = 1.5 Hz and 8.0 Hz, FlH). δ_C (126 MHz, $CDCl_3$): 39.9, 51.5, 58.9, 59.1, 67.1, 67.5, 69.8, 69.9, 70.8, 71.7, 71.9, 115.0, 120.2, 121.6, 121.9, 124.1, 124.4, 126.68, 126.72, 128.4, 133.9, 139.4, 139.5, 140.49, 140.53, 141.9, 142.2, 149.86, 149.94, 158.5. m/z [MALDI-TOF] anal. calcd 1666.9 (89%), 1667.9 (100%), 1668.9 (59%), 1669.9 (24%) and 1670.9 (8%). Found 1667.1 (88%), 1668.1 (100%), 1669.1 (62%), 1670.1 (25%), 1671.1 (9%). PLQY (solution) = 0.85 ± 0.01, PLQY (film) = 0.71 ± 0.05. T_g (100 °C min^{-1}) = 27 ± 1 °C (no melting transitions observed below 200 °C). $T_{5\%\ dec}$ = 399 °C. $E_{1/2}$ (Ox-1, CH_2Cl_2, Glassy C) = 0.87 V. GPC: $\bar{M}_n$ = 2026, $\bar{M}_w$ = 2037, $\bar{M}_v$ = 2035.

3,6-Bis{3,5-bis[4-(2-ethylhexyloxy)phenyl]phenyl}-9-[2-(2-methoxyethoxy)ethyl]carbazole (6b). 3,6-Dibromo-9-[2-(2-methoxyethoxy-)ethyl]carbazole **4b** (0.070 g, 0.136 mmol) and 2-{3,5-bis[4-(2-ethylhexyloxy)phenyl]phenyl}-4,4,5,5-tetramethyl-1,3,2-dioxaborolane **2**[41] (0.250 g, 0.408 mmol) were dissolved in toluene (3.0 cm^3). Aqueous potassium carbonate (2.0 M, 1.0 cm^3) and *tert*-butanol (1.0 cm^3) were added and the mixture was deoxygenated by sparging with nitrogen for 10 min. Tetrakis(triphenylphosphine)palladium(0) (0.009 g, 0.008 mmol) was added and the mixture was deoxygenated by sparging with nitrogen for 10 min. The mixture was stirred at 100 °C under nitrogen for 5 h before it was allowed to cool to room temperature. The mixture was diluted with toluene (20 cm^3) and water (20 cm^3) and the layers were separated. The aqueous layer was extracted with toluene (2 × 20 cm^3) and the combined organics were washed with water (2 × 20 cm^3) and brine (20 cm^3). The organics were dried over anhydrous magnesium sulfate and decanted. The magnesium sulfate was washed with additional toluene and the decanted organics combined before the volatiles were removed *in vacuo*. The crude residue was separated by column chromatography over silica in two stages: firstly the mixture was separated using dichloromethane/ethyl acetate/*n*-hexane (1 : 1 : 8) as eluent and secondly using a dichloromethane/toluene mixture (1 : 4) as eluent to yield **6b** as an off-white glassy solid (0.120 g, 59%). Found C, 82.5; H, 8.9; N, 1.2; $C_{85}H_{107}NO_6$ requires C, 82.4; H, 8.7; N, 1.1. λ_{max} (CH_2Cl_2/nm): 269 ($\log \varepsilon$/dm^3 mol^{-1} cm^{-1} 5.06), 289sh (4.96), 302sh (4.83), 320sh (4.40) and 350sh (3.34). δ_H (500 MHz, $CDCl_3$): 0.88–1.00 (24H, m, overlapping Ethylhexyl CH_3), 1.30–1.60 (32H, m, overlapping ethylhexyl CH_2), 1.74–1.80 (4H, m, ethylhexyl CH), 3.34 (3H, s, N(C$_2$H$_4$)O(C$_2$H$_4$)OCH_3), 3.46–3.48 (2H, m, N(C$_2$H$_4$)OCH$_2$CH_2-OCH$_3$), 3.57–3.59 (2H, m, N(C$_2$H$_4$)OCH_2CH$_2$OCH$_3$), 3.91–3.97 (10H, m, ethyhexyl OCH_2 and NCH$_2$CH_2O(C$_2$H$_4$)OCH$_3$), 4.61 (2H, br t, J = 6.0 Hz, NCH_2CH$_2$O(C$_2$H$_4$)OCH$_3$), 7.03 (8H, 1/2AA′BB′, surface PhH), 7.59 (2H, d, J = 8.5 Hz, CbzH), 7.66–7.70 (10H, m, overlapping branching and surface PhH), 7.84–7.85 (6H, m, overlapping branching PhH and CbzH), 8.46 (2H, d, J = 1.5 Hz, CbzH). δ_C (126 MHz, $CDCl_3$): 11.3, 14.3, 23.2, 24.0, 29.3, 30.7, 39.6, 43.6, 59.2, 69.5, 70.7, 71.1, 72.1, 109.5, 115.0, 119.2, 123.78, 123.84, 124.5, 125.8, 128.5, 133.0, 133.8, 140.8, 142.1, 143.1, 159.3. m/z [MALDI-TOF] anal. calcd 1237.8 (100%), 1238.8 (97%), 1239.8 (47%), 1240.8 (16%),

1241.8 (5%). Found 1237.9 (100%), 1238.9 (90%), 1239.9 (50%), 1240.9 (12%), 1241.9 (4%). PLQY (solution) = 0.15 ± 0.01, PLQY (film) = 0.25 ± 0.06. T_g (20 °C min^{-1}) = 26 ± 1 °C (no melting transitions observed below 200 °C). $T_{5\%\ dec}$ = 389 °C. $E_{1/2}$ (Ox-1, THF, Glassy C) = 0.69 V. GPC: $\bar{M}_n$ = 1598, $\bar{M}_w$ = 1605, $\bar{M}_v$ = 1604.

Spectroscopy

Photoluminescence (PL) spectra were recorded on a Jobin-Yvon Horiba Fluorolog Tau or a Jobin-Yvon Horiba Fluoromax 4 using a xenon lamp as an excitation source. Spectroscopic grade solvents were used for solution measurements. Solution PLQY measurements were measured relative to quinine sulfate in 0.5 M aqueous sulfuric acid (PLQY = 0.55).[50] PLQY values were determined from plots of absorbance *vs* integrated PL for the dendrimers relative to that of the quinine sulfate standard ($0.01 \leq A' \leq 0.10$). The standard errors in the gradients of these plots calculated by least squares regression were propagated using the chain rule to determine the error in PLQY. Thin film PLQY measurements were performed using the procedure described by Greenham *et al.*[51] Thin film samples on fused silica substrates were excited using the 325 nm output of a HeCd laser under nitrogen.

PL lifetime measurements for the bifluorene-based dendrimers **5a/b** were performed in tetrahydrofuran solutions using a Picoquant time correlated single photon counting (TCSPC) setup. The dendrimers were excited at 375 nm with ~70 fs pulses and a repetition rate of 80 MHz with the frequency doubled output of a Ti:sapphire laser. PL decays were measured at 395 nm with an instrument response function (IRF) of ~300 ps FWHM. The corresponding measurements for carbazole-based dendrimers **6a/b** were performed in toluene solutions using a Jobin-Yvon Horiba Fluorolog FL3-11 with a TCSPC module. The dendrimers were excited at 372 nm with 1.2 ns pulses and a repetition rate of 1 MHz with the output of a Horiba Scientific NanoLED pulsed diode light source. PL decays were measured at 400 nm with an IRF of ~1.5 ns FWHM. Due to the proximity of the detection/excitation wavelengths and the weaker PLQY of the carbazole dendrimers, scatter of the excitation beam was observed in the decays. The background signal was recorded using spectrophotometric grade toluene as a scatterer, which was subtracted from the observed data. The PL decays were fitted to single exponential decays convoluted with the IRF.

Thin film PL quenching measurements

Fused silica substrates (12 mm diameter) were cleaned in acetone, 2-propanol and toluene under ultrasonication prior to dendrimer deposition. Dendrimer films were spin coated from 10 mg cm^{-3} solutions in spectrophotometric grade toluene. Dendrimer solutions were pipetted onto the surface of the cleaned substrates until the surface was covered by the solution and the films were immediately spun at 2000 rpm for 1 min (acceleration = 2000 rpm s^{-1}). The following film thicknesses were measured by contact profilometry: **5a**, 44 ± 3 nm; **5b**, 43 ± 5 nm; **6a**, 47 ± 4 nm; and **6b**, 54 ± 7 nm. These thicknesses were determined from an average of nine measurements (three individual measurements on three separate films) and the errors indicate their standard deviation. The substrates were clamped in a custom built sample holder (internal volume ~40 cm^3) in a Jobin Yvon Horiba Fluorolog Tau fluorometer. The dendrimer film was placed on the opposite side of the substrate to the excitation source (excitation beam perpendicular to the substrate surface) and the PL was detected in front facing mode. The dendrimers were excited at 350 nm (bifluorene-based **5a/b**) or 320 nm (carbazole-based **6a/b**) and the PL was monitored at 400 nm in all cases. A flow of nitrogen (4000 cm^3 min^{-1} for DNB, DNT, and pNT injections and 1000 cm^3 min^{-1} for DMNB and NM injections) was established into the chamber from an aperture directly facing the film (carrier gas flow perpendicular to the film surface) and held constant throughout each measurement. The flow of nitrogen was controlled by a Bronkhorst EL-FLOW Select mass flow controller calibrated for nitrogen within the flow range 150–7500 cm^3 min^{-1}. After the apparatus was purged with nitrogen for 15 min the PL intensity of the films were monitored for a period of up to 1 h during which analyte vapours were injected. Analytes were introduced by manually injecting a known volume (between 0.1 and 25 cm^3) of nitrogen saturated with analyte vapour into the nitrogen carrier stream over 1 s. A digital metronome was used to aid with timekeeping. Cotton wool was placed inside the syringes at the outlet to prevent the injection of particles of analyte into the carrier gas flow. The syringes were primed with nitrogen and stoppered before they were allowed to saturate with analyte vapours at 22 °C for at least 16 h prior to injection. The approximate concentration of analyte introduced was estimated from the reported saturated vapour concentrations[13,14,39] and the dilution ratio of the analyte in the nitrogen carrier stream.

Thin film quenching constants, K, were determined from the gradients of F_0/F *vs.* quencher concentration plots and the errors quoted in these values are the standard errors for these gradients calculated by least squares regression. When the errors in injection time (±0.1 s) and injected volume (syringe size dependent) were propagated using the chain rule the relative error in the injected analyte concentrations was found to be ≤±20%. A relative error of 20% was ascribed to all injected analyte concentrations and thereby to the detection limit concentrations determined from the plots of F_0/F *vs.* [Q].

Acknowledgements

This work was supported by the Australian Research Council (DP0986838). AJC, HC and GT were supported by Endeavour International Postgraduate Research Scholarships and University of Queensland Research Scholarships. PLB is a University of Queensland Vice Chancellor's Research Focussed Fellow and PM the recipient of an Australian Research Council Discovery Outstanding Researcher Award. We acknowledge funding from the University of Queensland (Strategic Initiative – Centre for Organic Photonics & Electronics).

References

1 R. J. Colton and J. N. Russell, *Science*, 2003, **299**, 1324.
2 D. S. Moore, *Rev. Sci. Instrum.*, 2004, **75**, 2499.

3 D. S. Moore, *Sens. Imaging*, 2007, **8**, 9.
4 Y. Bhattacharjee, *Science*, 2008, **320**, 1416.
5 J. Köhler and R. Meyer, *Explosives*, VCH, Weinheim, 4th edn, 1993.
6 G. Strada, *Scientific American*, Nature Publishing Group, 1996, vol. 40.
7 A. W. Czarnik, *Nature*, 1998, **394**, 417.
8 J. Akhavan, *The Chemistry of Explosives*, The Royal Society of Chemistry, Cambridge, 2nd edn, 2004.
9 A. Makovky and L. Lenji, *Chem. Rev.*, 1958, **58**, 627.
10 D. E. G. Jones, R. A. Augsten and K. K. Feng, *J. Therm. Anal.*, 1995, **44**, 533.
11 S. B. Markofsky, *Nitro Compounds, Aliphatic. In Ullmann's Encyclopedia of Industrial Chemistry*, Wiley-VCH Verlag GmbH & Co. KGaA, 2000.
12 R. G. Ewing and C. J. Miller, *Field Anal. Chem. Technol.*, 2001, **5**, 215.
13 S. W. Thomas III, J. P. Amara, R. E. Bjork and T. M. Swager, *Chem. Commun.*, 2005, 4572.
14 J.-S. Yang and T. M. Swager, *J. Am. Chem. Soc.*, 1998, **120**, 11864.
15 J.-S. Yang and T. M. Swager, *J. Am. Chem. Soc.*, 1998, **120**, 5321.
16 S. J. Toal and W. C. Trogler, *J. Mater. Chem.*, 2006, **16**, 2871.
17 S. W. Thomas III, G. D. Joly and T. M. Swager, *Chem. Rev.*, 2007, **107**, 1339.
18 S. J. Toal, J. C. Sanchez, R. E. Dugan and W. C. Trogler, *J. Forensic Sci.*, 2007, **52**, 79.
19 T. Naddo, X. Yang, J. S. Moore and L. Zang, *Sens. Actuators, B*, 2008, **134**, 287.
20 Y. Salinas, R. Martinez-Manez, M. D. Marcos, F. Sancenon, A. M. Costero, M. Parra and S. Gil, *Chem. Soc. Rev.*, 2012, **41**, 1261.
21 Y. Che, D. E. Gross, H. Huang, D. Yang, X. Yang, E. Discekici, Z. Xue, H. Zhao, J. S. Moore and L. Zang, *J. Am. Chem. Soc.*, 2012, **134**, 4978.
22 C. J. Cumming, C. Aker, M. Fisher, M. Fok, M. J. la Grone, D. Reust, M. G. Rockley, T. M. Swager, E. Towers and V. Williams, *IEEE Geosci. Remote Sens. Lett.*, 2001, **39**, 1119.
23 D. Zhao and T. M. Swager, *Macromolecules*, 2005, **38**, 9377.
24 C. Zhang, Y. Che, X. Yang, B. R. Bunes and L. Zang, *Chem. Commun.*, 2010, **46**, 5560.
25 M. A. Ali, S. S. Y. Chen, H. Cavaye, A. R. G. Smith, P. L. Burn, I. R. Gentle, P. Meredith and P. E. Shaw, *Sens. Actuators, B*, 2015, **210**, 550.
26 H. Cavaye, A. R. G. Smith, M. James, A. Nelson, P. L. Burn, I. R. Gentle, S.-C. Lo and P. Meredith, *Langmuir*, 2009, **25**, 12800.
27 H. Cavaye, P. E. Shaw, A. R. G. Smith, P. L. Burn, I. R. Gentle, M. James, S.-C. Lo and P. Meredith, *J. Phys. Chem. C*, 2011, **115**, 18366.
28 G. Tang, S. S. Y. Chen, P. E. Shaw, K. Hegedus, X. Wang, P. L. Burn and P. Meredith, *Polym. Chem.*, 2011, **2**, 2360.
29 A. J. Clulow, P. L. Burn, P. Meredith and P. E. Shaw, *J. Mater. Chem.*, 2012, **22**, 12507.
30 P. E. Shaw, H. Cavaye, S. S. Y. Chen, M. James, I. R. Gentle and P. L. Burn, *Phys. Chem. Chem. Phys.*, 2013, **15**, 9845.
31 M. Cigánek, M. Dressler and J. Teplý, *Chromatographia*, 1989, **27**, 109.
32 C. F. Poole, Q. Li, W. Kiridena and W. W. Koziol, *J. Chromatogr. A*, 2001, **912**, 107.
33 W. Kiridena, W. W. Koziol and C. F. Poole, *J. Chromatogr. A*, 2001, **932**, 171.
34 A. Rose, Z. Zhu, C. F. Madigan, T. M. Swager and V. Bulovic, *Organic Light Emitting Materials and Devices X*, SPIE, 2006, vol. 6333, p. 63330Y.
35 A. Kumar, M. K. Pandey, R. Anandakathir, R. Mosurkal, V. S. Parmar, A. C. Watterson and J. Kumar, *Sens. Actuators, B*, 2010, **147**, 105.
36 G. He, G. Zhang, F. Lü and Y. Fang, *Chem. Mater.*, 2009, **21**, 1494.
37 S. Pramanik, C. Zheng, X. Zhang, T. J. Emge and J. Li, *J. Am. Chem. Soc.*, 2011, **133**, 4153.
38 B. Baez, S. N. Correa, S. P. Hernandez-Rivera, M. de Jesus, M. E. Castro, N. Mina and J. G. Briano, *Detection and Remediation of Mines and Minelike Targets IX*, SPIE, Bellingham WA, 2004, vol. 5415, p. 1389.
39 W. M. Jones and W. F. Giauque, *J. Am. Chem. Soc.*, 1947, **69**, 983.
40 H. Cavaye, P. E. Shaw, X. Wang, P. L. Burn, S.-C. Lo and P. Meredith, *Macromolecules*, 2010, **43**, 10253.
41 S.-C. Lo, E. B. Namdas, P. L. Burn and I. D. W. Samuel, *Macromolecules*, 2003, **36**, 9721.
42 A. J. Samson and J. A. Osaheni, *Science*, 1994, **265**, 765.
43 S. Dong, Z. Li and J. Qin, *J. Phys. Chem. B*, 2008, **113**, 434.
44 J. R. Lackowicz, *Principles of Fluorescence Spectroscopy*, Springer, New York, 3rd edn, 2006.
45 W. J. Aixill, P. B. Mills, R. G. Compton, F. Prieto and M. Rueda, *J. Phys. Chem. B*, 1998, **102**, 9187.
46 S. F. Alvarado, P. F. Seidler, D. G. Lidzey and D. D. C. Bradley, *Phys. Rev. Lett.*, 1998, **81**, 1082.
47 M. E. Fisher, M. La Grone and J. Sikes, *Detection and Remediation Technologies for Mines and Minelike Targets VIII*, SPIE, Orlando, FL, USA, 2003, vol. 5089, p. 991.
48 C.-H. Ku, C.-H. Kuo, C.-Y. Chen, M.-K. Leung and K.-H. Hsieh, *J. Mater. Chem.*, 2008, **18**, 1296.
49 C. J. Kelley, A. Ghiorghis, Y. Qin, J. M. Kauffman, J. A. Novinski and W. J. Boyko, *J. Chem. Res. (M)*, 1999, 0401.
50 G. A. Crosby and J. N. Demas, *J. Phys. Chem.*, 1971, **75**, 991.
51 N. C. Greenham, I. D. W. Samuel, G. R. Hayes, R. T. Phillips, Y. A. R. R. Kessener, S. C. Moratti, A. B. Holmes and R. H. Friend, *Chem. Phys. Lett.*, 1995, **241**, 89.